

Formation of germanium oxide microcrystals on the surface of Te-implanted Ge



J. Perrin Toinin^{a,b}, Y. Rudzevich^c, K. Hoummada^a, M. Texier^a, S. Bernardini^a, A. Portavoce^b, L. Chow^{c,*}

^aAix-Marseille Université, IM2NP, Faculté des Sciences et Techniques de Saint-Jérôme Case 142, 13397 Marseille, France

^bCNRS, IM2NP, Faculté des Sciences et Techniques de Saint-Jérôme Case 142, 13397 Marseille, France

^cDept. of Physics, University of Central Florida, Orlando, FL 32816, USA

ARTICLE INFO

Article history:

Received 30 September 2014

Received in revised form 13 April 2015

Accepted 15 July 2015

Available online 25 July 2015

Keywords:

Germanium
Ion implantation
Germanium oxide
Microcrystals

ABSTRACT

The formation of voids on the surface of heavily implanted germanium has been known for more than 30 years. Recently there is a renewed interest in germanium due to its potential application in the complementary metal oxide semiconductor (CMOS) devices. Here we report the observation of germanium oxide microcrystals formed on the surface of tellurium implanted into a germanium substrate. The Ge target used was a (100) polished single crystalline germanium wafer and the implantation was carried out at room temperature with Te ions at 180 keV and a fluence of 3.6×10^{15} at/cm². Under scanning electron microscope (SEM), the surface of the Ge substrate is evenly covered by microcrystals with a diameter about 1–2 μm and a coverage density of $\sim 10^7$ particles/cm². The initially smooth surface of the polished germanium substrate becomes very rough and mostly consists of voids with an average diameter of 40–60 nm, which is consistent with reports of heavily implanted germanium. The composition of the microcrystals was studied using energy dispersive X-ray analysis (EDX) and atom probe tomography (APT) and will be presented. Preliminary results indicate that tellurium is not detected in the microcrystals. The origin of the microcrystals will be discussed.

© 2015 Elsevier B.V. All rights reserved.

1. Introduction

In recent years there has been a renewed interest to incorporate germanium (Ge) in complementary metal oxide semiconductor (CMOS) devices. This focused attention on Ge is mainly due to Ge's higher carrier mobility and its compatibility with silicon (Si) technology. However unlike silicon [1], which has been intensively studied in the last 60 years, germanium is a material that is much less investigated in the past. Many fundamental doping and diffusion properties of impurities in germanium are still not well known [2]. For example, the best way to produce an effective n-doped germanium is still not known. The control of the enhanced diffusion of n-type dopants in germanium and their limited donor activation will be important for the fabrication of Ge-based electronic devices [3]. In addition, at the metal/Ge interface, the reduction of Schottky barrier height is an important issue for the realization of high performance Ge based devices [4].

Traditionally ion implantation has been the method of choice to dope semiconducting electronic devices since the mid 1970 [5]. For

germanium, it has been shown [6] that self-ion bombardment of a fluence above 2×10^{15} ions/cm² produced a cellular structure that consists of nano-cavities with average radius of 50 nm. Several research groups have investigated this phenomenon [7,8].

In an effort to develop new methodology for n-type doping of germanium, we investigate the effect of Te n-doping of germanium using ion implantation. Te ion implantation has been used to study radiation defects and possible use as n-type dopants in semiconductors in the past. Mayer, Marsh et al. [9], used Te and Zn ion implantation to form n-type and p-type layers in GaAs substrates. Orel [10] has studied radiation damages and defects in silicon due to Te ion implantation. Pashov et al. [11], investigated radiation damages and defects in Te ion implanted germanium crystals, while Wilson, Zavada et al. [12], studied the redistribution and activation of Te ion implanted GaN substrates. Here we report the observation of formation of micro-crystals of GeO_x during the room temperature Te ion implantation.

2. Materials and methods

Germanium wafer with (100) orientation is implanted with 180 keV Te ions at a fluence of 3.60×10^{15} at/cm² at room

* Corresponding author.

E-mail address: Lee.Chow@ucf.edu (L. Chow).

temperature. The ion implantation was carried out by Ion Beam Service*. After implantation, the Ge substrates were annealed at 700 °C, 650 °C, 600 °C, 550 °C, 500 °C, 450 °C for time intervals ranging from 1 h to 192 h. Then the Ge samples were characterized by secondary ion mass spectrometry (SIMS), scanning electron microscopy (SEM), energy dispersive X-ray analysis (EDX), transmission electron microscopy (TEM), and atom probe tomography (APT) to understand the effects of ion implantation and thermal annealing. The results of the SIMS will be presented elsewhere [13] and will not be discussed here. All samples described in this report are from the same batch, except specifically described otherwise.

The surface morphology of the Ge is examined using a Zeiss ULTRA-55 FEG field emission scanning electron microscope. This SEM is equipped with a Noran system 7 EDS system for composition analysis. The transmission electron microscope used to examine the cross-section is an FEI Titan 80–300 Cs-corrected microscope operating at 200 kV or 300 kV. APT specimens were prepared by focused ion beam (FIB) in a FEI dual beam Helios NanoLab 600 via the liftout technique [14]. The micro-tips were prepared by means of the annular milling method [15] to obtain an end radius of ≈ 100 nm. APT analyses were performed with a CAMECA LEAP 3000 \times HR at a specimen temperature of 25 K, a 100 kHz picosecond laser pulses with an energy of 1.5 nJ, an evaporation rate of 0.002 ions pulse $^{-1}$ and a pressure of $< 2 \times 10^{-11}$ Torr. Data reconstruction was performed using IVASTM 3.6.2 software.

3. Results and discussion

3.1. Scanning electron microscopy

After implantation, the surface morphology of the samples was examined with a scanning electron microscope. In Fig. 1, the low

and high magnification SEM images of the as-implanted Ge sample and 600 °C annealed sample are shown. As we can see in Fig. 1(a) and (c), the surface of the Ge substrate is now evenly covered with 1–2 μm size microcrystals with a coverage density of 10^7 per cm^2 . The origin of these microcrystals is not clear at this moment. Presumably, it could come from the re-deposition of the sputtered Ge ions. However, Selenium ion implanted Ge wafer under similar condition did not yield any microcrystals on the surface of the Ge substrate [13]. In Fig. 1(b) and (d), with a higher magnification, we can see that the surface of the Ge substrate is consisted of nano-crystallites with an average size of 40–50 nm. It seems that the 1 h annealing at 600 °C does not seem to affect either the microcrystals or nano-crystallites.

3.2. Energy dispersive X-ray analysis

In order to find out the composition of these micro-crystals, we carried out EDX measurements inside the SEM chamber. The accelerating voltage used is 15 kV and a magnification of 5000 \times is used. In Fig. 2(a) the conventional SEM image is shown. In the EDX mode, we can either detect the Ge L X-ray, or O K X-ray. The results are shown in Fig. 2(b) and (c). We can see that when detecting Ge L X-ray, the Ge signals from the microcrystals or from the substrate are similar so we cannot distinguish the location or shape of the microcrystals in Fig. 2(b). However in Fig. 2(c), the location and the shape of the microcrystals are clearly visible. From these preliminary un-calibrated results, we tentatively assign the composition of the microcrystals to be GeO_x with $x = 1.9$.

3.3. Transmission electron microscopy

Cross sectional TEM sample was prepared after coated the Te-implanted Ge substrate with a thin Pt protective film. The sample used here has the same fluence and implantation energy as

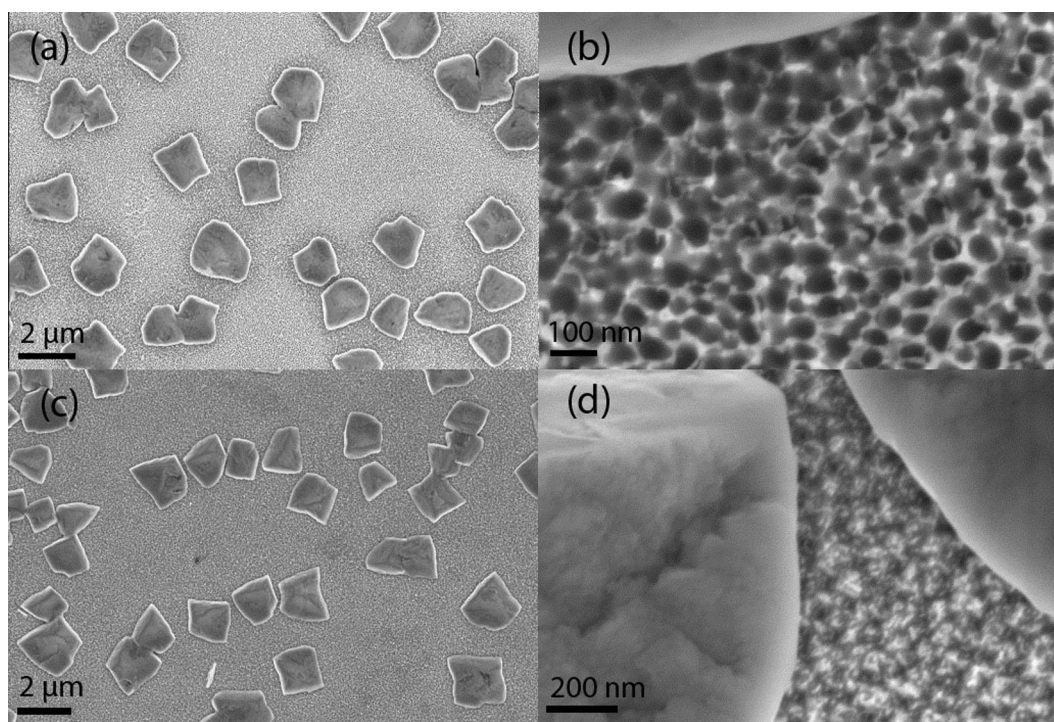


Fig. 1. (a) SEM image of low magnification as-implanted Te \rightarrow Ge sample, scale bar = 2 μm . (b) SEM image of high magnification as-implanted Te \rightarrow Ge sample, scale bar = 100 nm. (c) SEM image of low magnification, 600 °C annealed Te \rightarrow Ge sample, scale bar = 200 nm. (d) SEM image of high magnification, 600 °C annealed Te \rightarrow Ge sample, scale bar = 200 nm.

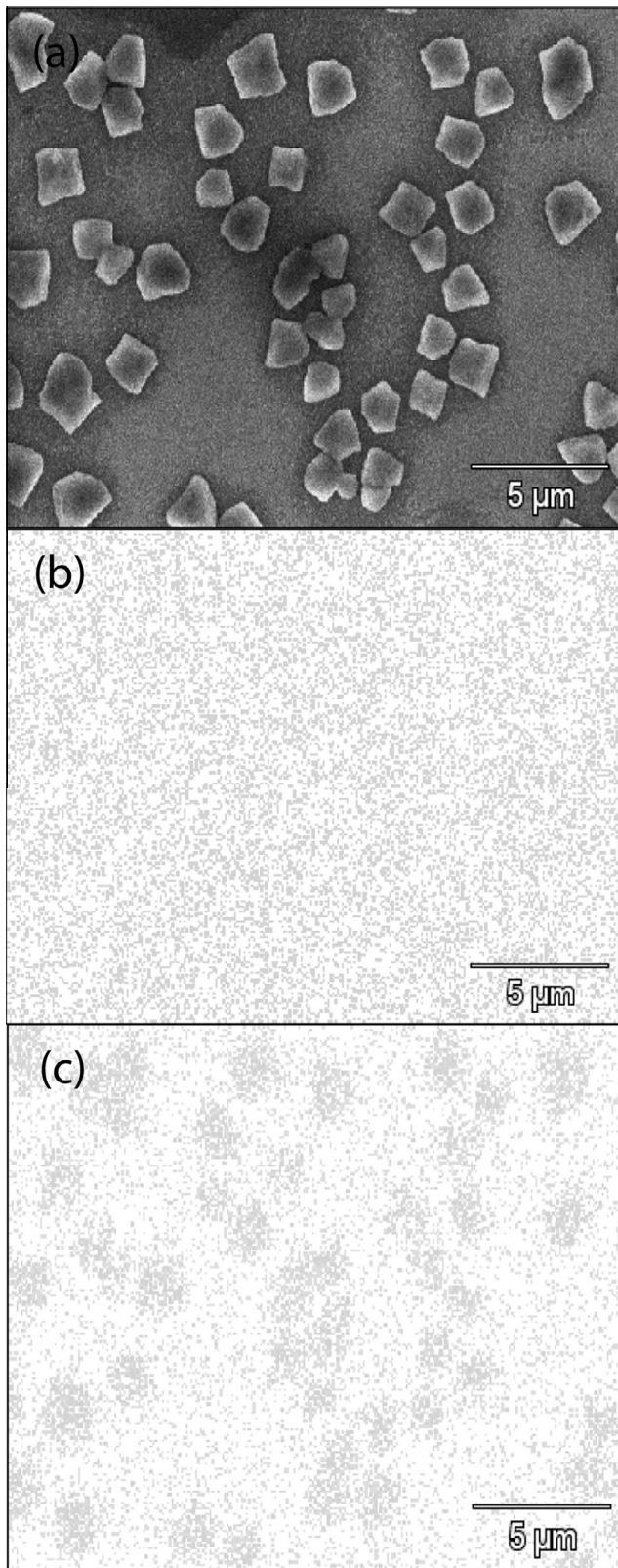


Fig. 2. (a) SEM image of as-deposited Te in Ge. (b) EDX image of the same region as in (a) using Ge L X-ray. (c) EDX image of the same region as in (a) using O K X-ray.

described above and it has been annealed at 650 °C for 1 h. We hope to capture XTEM images of the GeO_x microcrystals. Unfortunately our XTEM images showed no GeO_x microcrystals.

It is possible that the sample preparation procedures could exclude or dislodge the microcrystals. In Fig. 3, two high resolution XTEM images of the implanted Ge substrate are shown. In Fig. 3(a), on the Pt/Ge interface, a 50 nm size GeO_x nucleation site is formed. In Fig. 3(b), a high resolution image of a nucleation site is shown.

In an attempt to understand the formation of GeO_x microcrystals on the Ge substrate, we prepared a sputter deposited Ge film (340 nm) on a silicon wafer which is covered with a native oxide layer. The sample is rapid thermal annealed at 600 °C for 20 min and then implanted with 130 keV Se ions to a fluence of 3.6×10^{15} at/cm². The sample is then annealed at 525 °C for 168 h. Cross sectional TEM sample was prepared using the FIB liftout technique. In Fig. 4, we noticed that GeO_x clusters similar to the microcrystals observed in Fig. 3 are also presented. These GeO_x clusters have a diameter of 200–400 nm. They are typically embedded in the Ge film and partially exposed on the surface. The TEM observations show in this case that the GeO_x clusters are amorphous.

3.4. Atom probe tomography

The APT analysis provides us with information on the composition of the GeO_x micro-crystals. The analysis presented doesn't represent the full cluster from the top to the Ge substrate surface, consequently, information about the depth of the cluster is not well defined.

Fig. 5 presents a top view of the APT measurement of a GeO_x micro-crystal on the Te-implanted crystalline germanium substrate. The grey points represent various types of germanium oxide clusters from a stoichiometry of 66% of germanium (Ge_2O) to a stoichiometry of 33% of germanium (GeO_2). On the other hand, the black points represent single germanium atoms. We can see that the structure of the GeO_x micro-crystal is not homogenous and it can be classified on this reconstruction into two regions: an oxygen rich region and a pure germanium region. Note that the presence of tellurium atoms was not detected in this sample, because their concentration is much below Ge or O concentrations.

Fig. 6 presents the concentration profile of an oxide rich region from the top to the bottom of the cluster. It can be observed a concentration corresponding to the GeO compound on the top of the cluster and then gradually reduces to GeO_x with $x = 0.20$. It is important to note that concentration profile does not correspond to the full cluster depth. When comparing with the EDX data mentioned above, we should point out that EDX data are not calibrated, so APT results should be closer to the true values of Ge concentration inside the GeO_x microcrystals.

4. Summary

Pattern formation on ion beam irradiated surfaces has been well known for more than 60 years [16]. However, to the best of our knowledge, the formation of micron-size GeO_x crystals due to ion beam bombardment has not been observed in the past. We observed the formation of GeO_x micro-crystals on the Te ions implanted Ge monocrystalline substrate after implanted with 180 keV Te ions at a fluence of 3.6×10^{15} at·cm⁻². However, for the same Ge substrate implanted with 130 keV Se ions at the same fluence, we did not observe any GeO_x micro-crystals. At this moment, the detail mechanism of the formation of these micro-crystals is not known. It is also not clear what is the origin of the oxygen detected in the micron-size GeO_x crystals. It is believed that the native oxide layer [17] on the Ge monocrystalline substrate could be the origin of the oxygen in the GeO_x crystals. As we mentioned earlier that Ge monocrystalline substrates are quite susceptible ion bombardment. At fluence above 2×10^{15} ions/cm²

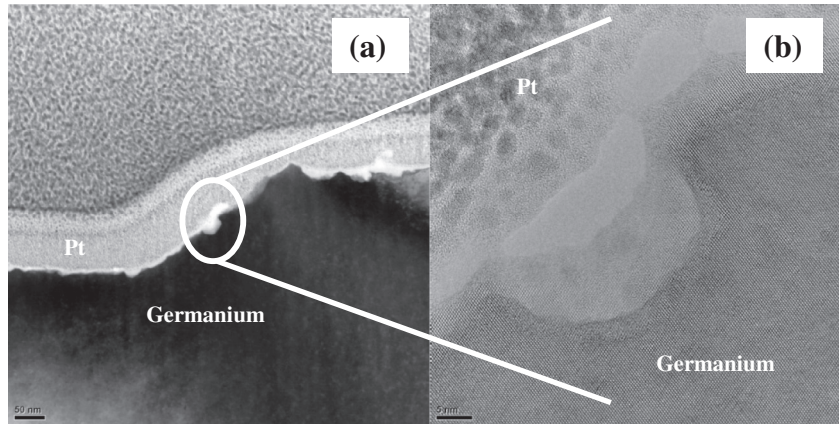


Fig. 3. Cross sectional TEM image of Te ion implanted Ge substrate. (a) Scale bar = 50 nm, magnification = xxxx. (b) Scale bar = 5 nm, magnification = yyyy.

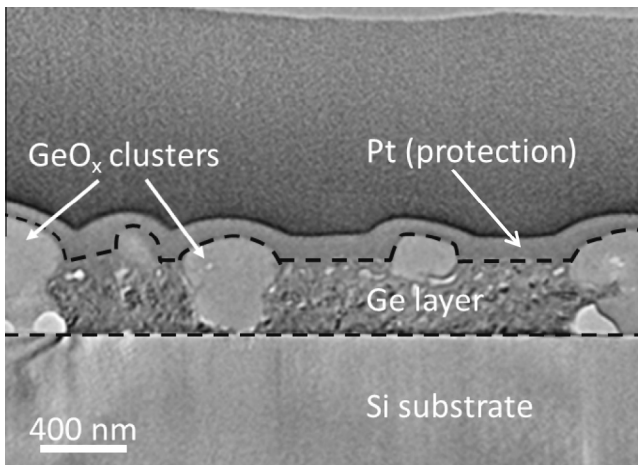


Fig. 4. Cross sectional TEM image of germanium layer implanted with 130 keV selenium ions with a dosage of 3.6×10^{15} at/cm² and annealed at 525 °C for 7 days. We can see clearly the formation of GeO_x clusters with a diameter of 200–400 nm.

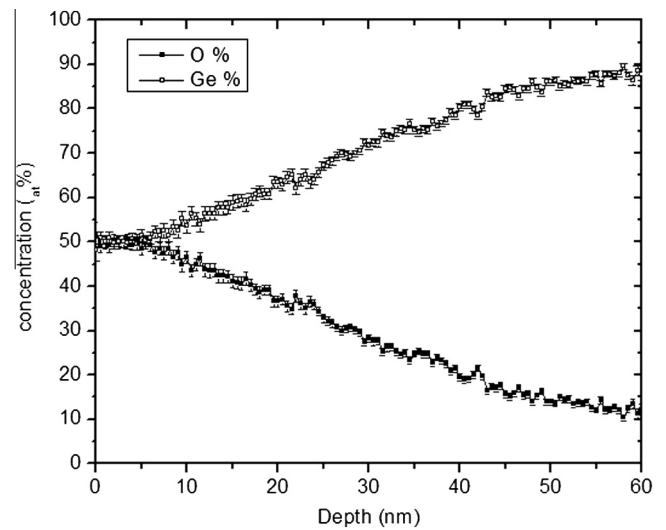


Fig. 6. Germanium and oxygen concentration as a function of the depth.

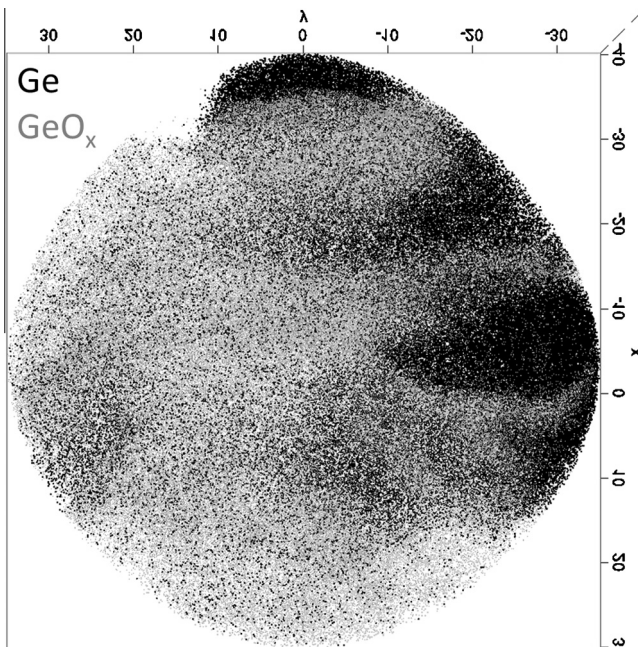


Fig. 5. Top view of APT analysis of a GeO_x cluster on mono-crystalline germanium sample. Grey points correspond to germanium oxide molecules and black points correspond to Ge atoms.

will produce a cellular structure on the surface of the germanium. This property combined with (a) the large quantity of defects such as vacancies and interstitials, created during the ion implantation, and (b) the high diffusion rate of defects in irradiated Ge substrate, may result in the formation of GeO_x micro-crystals.

References

- [1] Diffusion in silicon: ten years of research, in: D.J. Fisher (Ed.), Defect and Diffusion Forum, vols. 133–135, 1998, Scitec Publications.
- [2] J. Vanhellemont, E.R. Simoen, J. Electrochem. Soc. 154 (2007) H572–H583.
- [3] H. Bracht, S. Schneider, R. Kube, Microelectron. Eng. 88 (2007) 452.
- [4] A. Dimoulas, P. Tsipas, A. Sotiropoulos, E.K. Evangelou, Appl. Phys. Lett. 89 (2006) 252110.
- [5] E. Chason, S.T. Picraux, et al., J. Appl. Phys. 81 (1997) 6513.
- [6] I.H. Wilson, J. Appl. Phys. 53 (1982) 1698.
- [7] O.W. Holland, B.R. Appleton, J. Narayan, J. Appl. Phys. 54 (1983) 2295.
- [8] P. Bellon, S.J. Chey, J.E. Van Norstrand, M. Chaly, D.G. Cahill, R.S. Averback, Surf. Sci. 339 (1995) 135.
- [9] J.W. Mayer, O.J. Marsh, R. Mankavious, R. Bower, J. Appl. Phys. 38 (1967) 1975.
- [10] V. Orel, Czechoslovak J. Phys. 25 (1975) 376.
- [11] N. Pashov, S. Simov, M. Kalitzova, M.G. Michailov, A. Djakov, Phys. Stat. Solidi (a) 55 (1979) 599.
- [12] R.G. Wilson, J.M. Zavada, et al., J. Vac. Sci. Technol. A 17 (1999) 1226.
- [13] J. Perrin Toinin, A. Portavoce, K. Hoummada, M. Texier, M. Bertoglio, S. Bernardini, L. Chow, Beilstein J. Nanotechnol. 6 (2015) 336–342.
- [14] K. Thompson, D. Lawrence, D. Larson, J. Olson, T. Kelly, B. Gorman, Ultramicroscopy 107 (2007) 131–139.
- [15] D. Larson, D. Foord, A. Petford-Long, H. Liew, M. Blamire, A. Cerezo, G. Smith, Ultramicroscopy 79 (1999) 287–293.
- [16] W.L. Chan, E. Chason, J. Appl. Phys. 101 (2007) 121301.
- [17] P.W. Wang, Y. Qi, D.O. Henderson, J. Non-crystall. Solids 224 (1998) 31–35.